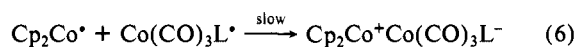
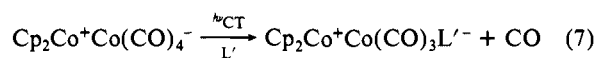


conversion of  $\text{Co}(\text{CO})_4^*$  to  $\text{Co}(\text{CO})_3\text{L}^*$  minimizes the energy wasting back electron transfer

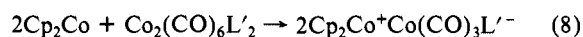


owing to the significantly enhanced oxidation potential of the phosphine-substituted radical.<sup>14</sup> Indeed the high quantum yield ( $\Phi = 0.3$ ) for the photoredox process (eq 4) indicates that  $\text{Co}(\text{CO})_4^*$  is scavenged by phosphine half as fast as it undergoes back electron transfer in eq 3. Furthermore the interception of  $\text{Co}(\text{CO})_4^*$  must follow cage escape from  $\text{Cp}_2\text{Co}^*$  (see eq 3) since the ligand substitution of  $17\epsilon$  carbonylmetal radicals ( $k_s \sim 10^7 \text{ M}^{-1} \text{ s}^{-1}$ )<sup>15</sup> is generally slower than diffusive separation of radical pairs ( $\tau \sim 10^{-9} \text{ s}$ ).<sup>16</sup>

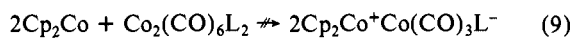
When phosphites such as  $\text{L}' = \text{P}(\text{OMe})_3$  and  $\text{P}(\text{OPh})_3$  are employed as scavengers, the stoichiometry of the photoinduced process is



which corresponds to an overall ligand substitution of the tetra-carbonylcobalt anion. Such a transformation also derives from an initial CT excitation of the CIP in eq 3 and ligand substitution by phosphite (cf. eq 5). Independent experiments demonstrate that the subsequent thermal reduction of the phosphite-substituted carbonylcobalt dimer is rapid and quantitative, i.e.



The latter illustrates the ligand dependence of the redox properties of carbonylmetals since the phosphine analogues are inert, i.e.<sup>19</sup>



These photoinduced processes of CIP thus provide a novel mode for the activation of ionic species in solution. We hope that further elaborations with a variety of other organometallic and organic ions will establish the generality of the charge-transfer methodology.

**Acknowledgment.** We thank J. D. Korp for crystallographic assistance and the National Science Foundation and Robert A. Welch Foundation for financial support.

**Supplementary Material Available:** Tables of bond distances and angles and anisotropic thermal parameters for  $\text{Cp}_2\text{Co}^+\text{Co}(\text{CO})_4^-$  (1 page); table of structure factor amplitudes (4 pages). Ordering information is given on any current masthead page.

(13) (a) Mugnier, Y.; Reeb, P.; Moise, C.; Laviron, E. *J. Organomet. Chem.* **1983**, *254*, 111. (b) Reeb, P.; Mugnier, Y.; Moise, C.; Laviron, E. *J. Organomet. Chem.* **1984**, *273*, 247. (c) Wegman, R. W.; Brown, T. L. *Inorg. Chem.* **1983**, *22*, 183. (d) Cf. also: Lee, K. Y.; Kuchynka, D. J.; Kochi, J. K. *Organometallics* **1987**, *6*, 1886.

(14) For  $\text{Co}(\text{CO})_4^*$ ,  $\text{Co}(\text{CO})_3\text{PMe}_2\text{Ph}^*$ , and  $\text{Co}(\text{CO})_3[\text{P}(\text{OPh})_3]^*$ ,  $E^\circ_{\text{red}}$  are estimated to be +0.4, -0.4, and 0.0 V, respectively.

(15) (a) Fox, A.; Malito, J.; Poë, A. *J. Chem. Soc., Chem. Commun.* **1981**, 1052. (b) Hershberger, J. W.; Klingler, R. J.; Kochi, J. K. *J. Am. Chem. Soc.* **1983**, *105*, 61. (c) Herrinton, T. R.; Brown, T. L. *J. Am. Chem. Soc.* **1985**, *107*, 5200. (d) Summers, D. P.; Luong, J. C.; Wrighton, M. S. *J. Am. Chem. Soc.* **1981**, *103*, 5238. (e) Meyer, T. J.; Caspar, J. V. *Chem. Rev.* **1985**, *85*, 187.

(16) (a) Noyes, R. M. *Prog. React. Kinet.* **1961**, *1*, 129. (b) The unexpectedly slow rate of back electron transfer in spite of the driving force<sup>14,17</sup> may arise from a sizeable reorganization energy for  $\text{Co}(\text{CO})_4^*$  resulting from a configurational change.<sup>18</sup>

(17)  $E^\circ_{\text{ox}} = -0.95 \text{ V}$  for  $\text{Cp}_2\text{Co}$ . Koelle, U. *J. Organomet. Chem.* **1978**, *152*, 225.

(18) Hanlan, L. A.; Huber, H.; Kündig, E. R.; McGarvey, B. R.; Ozin, G. A. *J. Am. Chem. Soc.* **1975**, *97*, 7054. See, also: Elian, M.; Hoffmann, R. *Inorg. Chem.* **1975**, *14*, 1058.

(19) (a) The irreversible cathodic CV peak potential for  $\text{Co}_2(\text{CO})_6[\text{P}(\text{OPh})_3]_2$  is 300 mV more positive than that for  $\text{Co}_2(\text{CO})_6[\text{PMe}_2\text{Ph}]_2$ . (b) It is also possible<sup>14</sup> that  $\text{Co}(\text{CO})_3[\text{P}(\text{OPh})_3]^*$  is reduced by  $\text{Cp}_2\text{Co}^*$  prior to dimerization in eq 5.

## An Iron-Activated Alcohol Dehydrogenase: Metal Dissociation Constants and Magnetic and Spectroscopic Properties

Peter Tse, Robert K. Scopes, and Anthony G. Wedd\*

Departments of Chemistry and Biochemistry  
La Trobe University  
Bundoora, Victoria, 3083, Australia

Eddy Bakshi and Keith S. Murray\*

Department of Chemistry, Monash University  
Clayton, Victoria, 3168, Australia

Received August 12, 1987

Two alcohol dehydrogenases (ADH) have been isolated from the fermenting bacterium *Zymomonas mobilis*.<sup>1</sup> One is a "normal" zinc enzyme while the second contains iron ( $\alpha_4$ ; 150 000 Da). The presence of naturally occurring iron at the active center of an ADH or of any  $\text{NAD}^+$ -linked dehydrogenase has not been reported previously. In striking contrast to the four-coordinate  $\text{ZnN}_2\text{S}_2$  site in horse liver ADH,<sup>2</sup> this communication shows the center to be a mononuclear six-coordinate high spin ferrous site bound to oxygen and nitrogen ligand atoms. Preliminary spectroscopic and magnetic properties of the active  $\text{Fe}^{2+}$  and  $\text{Co}^{2+}$  forms are presented as well as those of the inactive  $\text{Mn}^{2+}$ ,  $\text{Fe}^{3+}$ ,  $\text{Ni}^{2+}$ ,  $\text{Cu}^{2+}$ , and  $\text{Zn}^{2+}$  forms.

The  $\text{Fe}^{\text{II}}$ -ADH is not very stable as isolated ( $t_{1/2}$ , 2–5 h; 4 °C). Inclusion of  $\text{Co}^{2+}$  in the isolation buffer provides  $\text{Co}^{2+}$ -substituted enzyme, Co-ADH, which is more stable and also active.<sup>3</sup> Treatment of Co-ADH with 1,10-phenanthroline leads to metal-free apoenzyme<sup>3</sup> which may be stored indefinitely at 77 K.  $\text{Fe}^{2+}$  and  $\text{Co}^{2+}$  reactivate apo-ADH completely<sup>3</sup> upon addition of a single equivalent, while  $\text{Zn}^{2+}$  is ineffective under the same conditions.

Apparent dissociation constants determined by metal buffer or competition experiments<sup>4</sup> are listed below

M:	$\text{Mn}^{2+}$	$\text{Fe}^{2+}$	$\text{Fe}^{3+}$	$\text{Co}^{2+}$	$\text{Ni}^{2+}$	$\text{Cu}^{2+}$	$\text{Zn}^{2+}$
$\text{p}K_{\text{M}}$ :	7.4	7.5	5.8	7.8	8.3	8.5	9.0

All the bivalent metals are tightly bound with  $\text{p}K_{\text{M}}$  increasing monotonically but slowly across the first transition series, a property generally associated with the presence of oxygen ligands.<sup>5</sup> The slope is even lower than those observed<sup>6</sup> for glyoxalase I and phosphoglucomutase, two enzymes thought to involve six-coordinate  $\text{N}_2\text{O}_4$  coordination spheres.

The tight metal binding and availability of apoenzyme to act as reference and as diamagnetic correction has facilitated spectral

(1) (a) Scopes, R. K. *FEBS Lett.* **1983**, *156*, 303–306. (b) Neale, A. D.; Scopes, R. K.; Kelly, J. M.; Wettenhall, R. E. *Eur. J. Biochem.* **1986**, *154*, 119–124. (c) Kinoshita, S.; Kakizono, T.; Kadota, K.; Das, K.; Taguchi, H. *Appl. Microbiol. Biotechnol.* **1985**, *22*, 249–254.

(2) Zeppezauer, M. In *The Coordination Chemistry of Metalloenzymes*; Bertini, I., Drago, R. S., Luchinat, C., Eds.; Reidel: Dordrecht, 1983; pp 99–122.

(3) Conditions: KMes (10 mM); pH 6.5. The specific activities of Fe-, Co-, and apo-ADH were 750, 300, and <3 IU  $\text{mg}^{-1}$ . Content (g atoms per subunit) of Fe, Co, and Zn, in the three forms were (0.96 ± 0.15, <0.05, <0.01), (<0.08, 1.16 ± 0.03, <0.01), and (<0.02, <0.05, <0.01), respectively. Enzyme concentrations in the range 0.6–1.2 mM were employed in the physical measurements.

(4)  $\text{p}K_{\text{Co}}$  was determined employing nitrilotriacetic acid as metal buffer.<sup>6a</sup> The concentration of Co-ADH was estimated via the activity assay.  $\text{Fe}^{2+}$  oxidized under the above conditions.  $\text{p}K_{\text{M}}$  for the inactive M-ADH (M =  $\text{Mn}^{2+}$ ,  $\text{Ni}^{2+}$ ,  $\text{Cu}^{2+}$ ,  $\text{Zn}^{2+}$ ) were determined via competition with  $\text{Co}^{2+}$ . Complementary experiments in which total  $\text{Co}^{2+}$  and then total  $\text{M}^{2+}$  concentrations were kept constant were employed to maximize precision. The constant for  $\text{Fe}^{2+}$  was established via competition with  $\text{Zn}^{2+}$  and that for  $\text{Fe}^{3+}$  via competition with  $\text{Fe}^{2+}$ .

(5) Sigel, H.; McCormick, D. M. *Acc. Chem. Res.* **1970**, *3*, 201–208.

(6) (a) Sellin, S.; Mannervik, B. *J. Biol. Chem.* **1984**, *259*, 11426–11429, and references therein. (b) Ray, W. J., Jr. *J. Biol. Chem.* **1969**, *244*, 3740–3747.

and magnetic characterization of the system.

Fe<sup>II</sup>-ADH (95.4 atom% <sup>57</sup>Fe) shows a single, asymmetric quadrupole doublet in its Mossbauer spectrum at 4.2 K. The isomer shift ( $\delta$ , 1.24 mm s<sup>-1</sup>) and quadrupole splitting ( $\Delta E_Q$ , 3.43 mm s<sup>-1</sup>) are typical of high spin  $S = 2$  ferrous centers in a ligand field of symmetry close to octahedral.<sup>7</sup> In the presence of a 3.2 T magnetic field, a broad, poorly resolved spectrum was obtained. The spin state is confirmed by the temperature dependence of the magnetic susceptibility measured in the range 4.3–50 K on a SQUID susceptometer (Figure 1): A Curie-Weiss dependence is observed ( $\theta$ , -3.5 K) with  $\mu_{Fe} \sim 5.4 \mu_B$  in the range 50–20 K and decreasing to 4.1  $\mu_B$  at 4.3 K. The behavior is that expected for a <sup>5</sup>T<sub>2</sub>(d<sup>6</sup>) ground state, whose orbital degeneracy has been raised by moderate spin-orbit coupling and by a lower symmetry ligand field.<sup>8</sup>

Active Co<sup>II</sup>-ADH features a well-resolved electronic spectrum (Figure 2;  $\lambda_{max}$  510 nm,  $\epsilon$  31.5 M<sup>-1</sup> cm<sup>-1</sup>) whose molar absorptivity is characteristic of a high spin  $S = 3/2$  six-coordinate center of symmetry less than octahedral.<sup>9</sup> The spectrum is similar to those<sup>10</sup> of Co<sup>2+</sup>-substituted glyoxalase I, conalbumin, and phospholipase C. The magnetic moment shows a gradual decrease from 5.9  $\mu_B$  at 52.3 K to 3.9  $\mu_B$  at 4.2 K, behavior expected<sup>8</sup> for a <sup>4</sup>T<sub>1</sub>(d<sup>7</sup>) ground state influenced by similar spin-orbit coupling and ligand field effects to those acting in Fe<sup>II</sup>-ADH. The ESR spectrum ( $g_1$ , 5.60;  $g_2$ , 3.98;  $g_3$ , 2.55;  $g_{av}$  4.04)<sup>11</sup> at 9.5 K supports the presence of a distortion away from octahedral symmetry. The absence of strong absorptions above 350 nm in the electronic and MCD<sup>12</sup> spectra indicates that cysteine is not a ligand.

Each of these physical techniques detect changes at the cobalt site in the binary Co<sup>II</sup>-ADH-NAD<sup>+</sup> and ternary Co<sup>II</sup>-ADH-NAD<sup>+</sup>-*i*-PrOH complexes<sup>13</sup> (e.g., Figure 2). *i*-PrOH has no effect in the absence of NAD<sup>+</sup>. Subtle changes only are apparent in the 4.2 K Mossbauer parameters of the Fe<sup>II</sup>-binary and -ternary complexes.

The data for Mn<sup>II</sup>, Ni<sup>II</sup>, and Cu<sup>II</sup>-ADH support the presence of high spin  $S = 5/2$ , 1, and  $1/2$  sites, respectively. In particular, the ESR spectrum of Cu<sup>II</sup>-ADH (Figure 3)<sup>11,14</sup> exhibits a well-resolved nine-line hyperfine pattern in the  $g_{\perp}$  region, characteristic of the presence of four <sup>14</sup>N ( $I = 1$ ) ligand atoms, probably supplied by histidine residues.<sup>15</sup> Mn<sup>II</sup>-ADH shows a strict Curie temperature dependence with  $\mu_{Mn}$ , 5.9  $\mu_B$ , and a high spin Mn<sup>II</sup> ESR spectrum<sup>14</sup> similar to that of manganese(II)-phosphoglucumutase.<sup>16</sup>

It is apparent from the existing data that the metal binding site contains a mixture of nitrogen and oxygen ligand atoms and that, for the native enzyme, a mononuclear high spin ferrous site is present. Certain oxygenase systems,<sup>17</sup> such as lipoxygenase I and

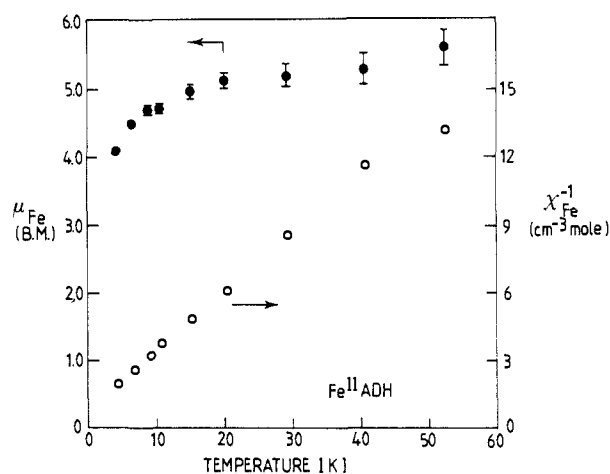


Figure 1. Temperature dependence of the reciprocal magnetic susceptibility (O) and of the magnetic moment (●) per iron atom for Fe<sup>II</sup>-ADH.

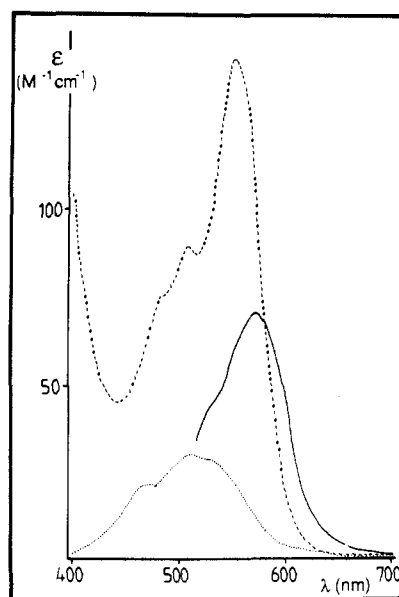


Figure 2. Limiting electronic spectra of Co<sup>II</sup>-ADH:<sup>3,13</sup> no additives, (···); enzyme plus NAD<sup>+</sup> (3.4 equiv), (—); enzyme plus NAD<sup>+</sup> (3.4 equiv) and *i*-PrOH (2600 equiv), (---).

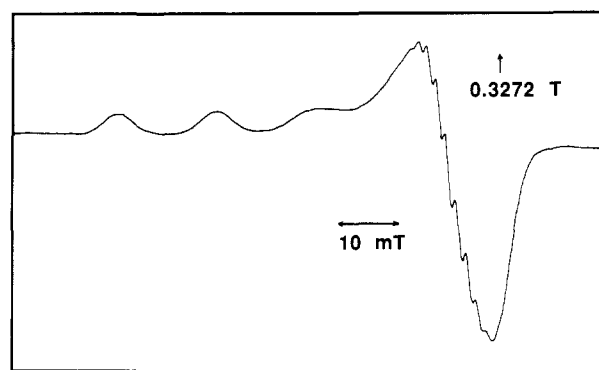


Figure 3. ESR spectrum of Cu<sup>II</sup>-ADH.<sup>3</sup>

catechol 2,3-dioxygenase, exhibit similar structural features: a closer comparison with those systems and with the zinc-based ADHs<sup>2</sup> will emerge from continuing work.

(7) (a) Johnson, C. E. *Topics Appl. Phys.* **1975**, *5*, 139–161. (b) Huynh, B. H.; Kent, T. A. *Adv. Inorg. Biochem.* **1985**, *6*, 163–223.

(8) Mabbs, F. E.; Machin, D. J. *Magnetism and Transition Metal Complexes*; Chapman and Hall: London, 1973; Chapter 5.

(9) Banci, L.; Bencini, A.; Benelli, C.; Gatteschi, D.; Zanchini, C. *Struct. Bonding* **1982**, *52*, 37–86.

(10) (a) Bertini, I.; Luchinat, C. *Adv. Inorg. Biochem.* **1985**, *6*, 71–111. (b) Bicknell, R.; Hanson, G. R.; Holmquist, B.; Little, C. *Biochem.* **1986**, *25*, 4219–4223. (c) Sellin, S.; Eriksson, L. E. G.; Aronsson, A.-C.; Mannervik, B. *J. Biol. Chem.* **1983**, *258*, 2091–2093.

(11) Hanson, G. R.; Pilbrow, J. R. are thanked for assistance.

(12) Bicknell, R.; Holmquist, B.; Scopes, R. K., unpublished observations.

(13) The molar ratios of oxidizing substrate NAD<sup>+</sup> and inhibitor *i*-PrOH of 3.4 and 2600 per subunit are those which generate limiting vis-UV and ESR spectra in the Co<sup>II</sup> system. Note that *i*-PrOH causes dissociation of the tetrameric enzyme into a dimer form.

(14) <sup>63</sup>Cu-ADH:  $g_{\parallel}$ , 2.275;  $g_{\perp}$ , 2.057;  $A_{\parallel}$ ,  $173 \times 10^{-4}$  cm<sup>-1</sup>;  $A_{\perp}$ ,  $15.3 \times 10^{-4}$  cm<sup>-1</sup>;  $A_{\parallel}(N)$ ,  $1.6 \times 10^{-4}$  cm<sup>-1</sup>;  $A_{\perp}(N)$ ,  $14 \times 10^{-4}$  cm<sup>-1</sup>. Mn-ADH:  $g_0$ , 2.04;  $A_0$ ,  $86 \times 10^{-4}$  cm<sup>-1</sup>; ZFS < 0.014 cm<sup>-1</sup>.

(15) Siddiqui, S.; Shepherd, R. E. *Inorg. Chem.* **1986**, *25*, 3869–3876.

(16) Reed, G. H.; Ray, W. J., Jr. *Biochem.* **1971**, *10*, 3190–3197.

(17) Feiters, M. C.; Aasa, R.; Malmstrom, B. G.; Slappendel, S.; Veldink, G. A.; Vliegthart, J. F. G. *Biochim. Biophys. Acta* **1985**, *831*, 302–305.

**Acknowledgment.** P.T. acknowledges the award of a Commonwealth Postgraduate Scholarship. E.B. and K.S.M. thank the National Research Fellowships Scheme and the Australian Research Grants Scheme for financial support.

### Carbocupration of Cyclopropene. A Novel Synthon of Cyclopropanone Enolate and Its Application to [3 + 2] and [3 + 2 + 2] Annulation

Eiichi Nakamura,\* Masahiko Isaka, and Satoshi Matsuzawa

Department of Chemistry, Tokyo Institute of Technology  
Meguro, Tokyo 152, Japan

Received October 23, 1987

We report here that organocuprates undergo extremely rapid addition across the double bond of the cyclopropanone ketal **1**<sup>1</sup> to produce a previously inaccessible synthon of cyclopropanone enolate **2**. The resultant cuprio cyclopropane **2** then reacts with various electrophiles to produce substituted cyclopropanone ketals **3**. The virtue of this carbocupration/trapping reaction, besides its novelty,<sup>2</sup> stems from its ability to quickly assemble functional groups on the cyclopropane ring<sup>2c</sup> that are useful for further transformation. Thus, the reaction has been developed into a two-step transformation of **1** to a five-membered ring in a [3 + 2] manner as well as to a remarkably efficient single-pot [3 + 2 + 2] construction of a seven-membered ring (Scheme I).

Success of such an addition/trapping sequence primarily depends on the efficiency of the addition of the organometallics to the cyclopropene double bond. Of various species examined,<sup>3a</sup> organocuprates were found suitable for the desired reaction scheme.<sup>3b</sup> For instance, quantitative addition of Me<sub>2</sub>CuLi (1.1 equiv) to the cyclopropene **1** occurred at -70 °C in 1 min (in ether, terminated by addition of MeOH) to afford the 2-methylcyclopropanone ketal **3a** (96% yield by quantitative GLC analysis; 71% isolated yield). When the reaction was quenched by D<sub>2</sub>O, a deuteriated cyclopropane **3b** was obtained. A characteristic high field <sup>1</sup>H NMR signal of the protio 2-methylcyclopropane **3a** (0.30 ppm), assigned to the C-3 proton cis to the C-2 methyl group,<sup>4</sup> was absent in the deuteriated product **3b**, indicating the cis disposition of the metal and the methyl group (i.e., R<sup>1</sup>) in the cuprio cyclopropane **2**.

Given the evidence of clean cis addition of the cuprate, we examined the trapping of the cuprio cyclopropane with carbon electrophiles. Thus, treatment of **1** with Me<sub>2</sub>CuLi (1.0 equiv) followed by addition of MeI (2.1 equiv)/HMPA (1.05 equiv) gave, after warming to 0 °C, cis-2,3-disubstituted cyclopropane **3c** in

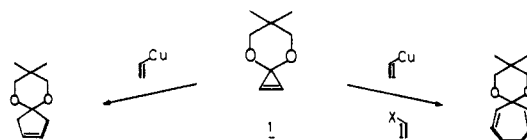
(1) Albert, R. M.; Butler, G. B. *J. Org. Chem.* **1977**, *42*, 674. Breslow, R.; Pecoraro, J.; Sugimoto, T. *Org. Synth.* **1977**, *57*, 41. For recent work on the thermal reaction of **1**, see: Boger, D. L.; Brotherton, C. E. *J. Am. Chem. Soc.* **1986**, *108*, 6695.

(2) (a) Carbometalation of simple olefins leading to stable organometallics has not been reported: Cf. Yamamoto, Y.; Yamada, J.-i.; Uyehara, T. *J. Am. Chem. Soc.* **1987**, *109*, 5820. (b) There have been reported a few examples of carbometalation of simple cyclopropenes by main group organometallics around or above room temperature: Grignard reagent: Lukina, M. Yu.; Rudashevskaya, T. Yu.; Nesmeyanova, O. A. *Dokl. Akad. Nauk SSSR* **1970**, *190*, 1109. Rudashevskaya, T. Yu.; Nesmeyanova, O. A. *Izv. Akad. Nauk SSSR Ser. Khim.* **1983**, 1821. Lehmkuhl, H.; Mehler, K. *Liebigs Ann. Chem.* **1978**, 1841. Allylic metals: Köster, R.; Arora, S.; Binger, P. *Angew. Chem., Int. Ed. Engl.* **1969**, *8*, 205. Stoll, A. T.; Negishi, E.-i. *Tetrahedron Lett.* **1985**, *26*, 5671. (c) Elaborate preparation of substituted cyclopropanes directed toward synthesis of complex molecules has been achieved with low level of stereocontrol: cf. Piers, E.; Morton, H. E.; Nagakura, I.; Thies, R. W. *Can. J. Chem.* **1983**, *61*, 1226. Wender, P. A.; Essenstat, M. A.; Filosa, M. P. *J. Am. Chem. Soc.* **1979**, *101*, 2196. Yamamoto, H.; Kitatanl, K.; Hiyama, T.; Nozaki, H. *J. Am. Chem. Soc.* **1977**, *99*, 5816.

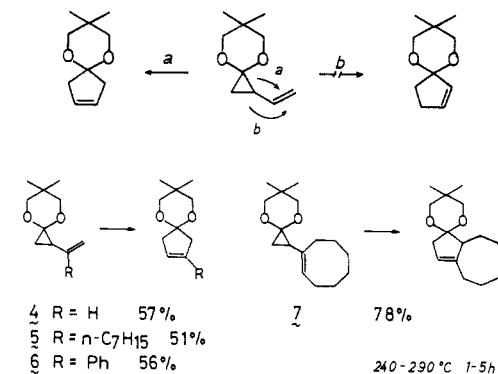
(3) (a) Reaction of alkyl lithium, alkylmagnesium halide, and alkylcopper resulted either in recovery of **1** at low temperatures or in total decomposition at higher temperatures. (b) The cuprio cyclopropane **2** starts to decompose above -50 to -20 °C.

(4) The assignment was based on the characteristically high chemical shift and the coupling constant (200 MHz <sup>1</sup>H NMR/CDCl<sub>3</sub> 0.30 ppm, dd, *J* = 5.4, 5.9 Hz): Cf. Jackman, L. M.; Sternhell, S. *Applications of Nuclear Magnetic Resonance Spectroscopy in Organic Chemistry*, 2nd ed.; Pergamon Press: Oxford, 1969; pp 227 and 286.

#### Scheme I



#### Scheme II<sup>a</sup>



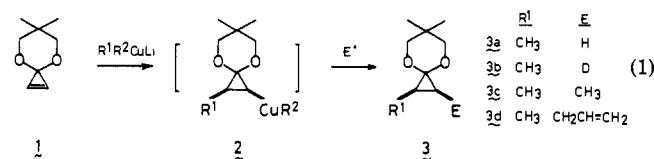
<sup>a</sup> Carried out in toluene containing 1 equiv of bis(trimethylsilyl)acetamide.

**Table I.** Carbocupration/Electrophilic Trapping of the Cyclopropanone **1**<sup>a</sup>

entry	cuprate (equiv)	electrophile (equiv)	product	yield <sup>b</sup>
1	Me <sub>2</sub> CuLi (1.10)	MeOH	<b>3a</b>	71, 96 <sup>c</sup>
2	(1.0)	MeI (2.1) / HMPA (1.05)	<b>3c</b>	88 <sup>c</sup>
3	(1.05)	CH <sub>2</sub> =CHCH <sub>2</sub> Br (2.1)	<b>3d</b>	81 <sup>d</sup>
4	MeCu≡SiMe <sub>3</sub> (1.05)	CH <sub>2</sub> =CHCH <sub>2</sub> Br (1.05)	<b>3d</b>	76 <sup>d</sup>
5	MeCuSPH (1.1)	MeI (1.0) / HMPA (1.1)	<b>3c</b>	78 <sup>c</sup>
6	Bu <sub>2</sub> CuLi (1.0)	BuI (2.1) / HMPA (1.05)	<b>3c</b>	72
7	R <sup>1</sup> R <sup>2</sup> CuLi (1.3)	H <sub>2</sub> O	<b>3a</b>	R = H 54
8	R <sup>1</sup> R <sup>2</sup> CuLi (1.3)	H <sub>2</sub> O	<b>3a</b>	R = Ph 78
9	Cu≡SiMe <sub>3</sub> (1.0)	H <sub>2</sub> O	<b>3a</b>	R = H 72
10	Cu <sub>2</sub> Li (1.1)	MeI (5) / HMPA (1.1)	<b>3c</b>	R = Me 79

<sup>a</sup> See footnote 14 for experimental procedure. <sup>b</sup> Isolated yield except in entries 1-5. <sup>c</sup> Determined by GLC by using an internal standard. <sup>d</sup> Determined by <sup>1</sup>H NMR by using an internal standard.

88% yield as a single product. Symmetry elements in the product, established by NMR spectroscopy,<sup>5</sup> unambiguously demonstrated the cis dimethyl structure. These experiments showed that the overall reaction (eq 1) involves the cis addition followed by the trapping with retention of the configuration.



The reaction proceeded smoothly for several combinations of cuprates and alkylating reagents. Table I summarizes the results of the addition/trapping sequence. Addition of Bu<sub>2</sub>CuLi followed by trapping with BuI afforded cis-dibutylcyclopropanone ketal (entry 6).<sup>5</sup> Allyl bromide reacted with the intermediary cuprio

(5) The appearance of only seven <sup>13</sup>C signals (equivalent ketal methyl groups as well as nonequivalent ketal methylene carbons) excluded the trans structure (C<sub>2</sub> symmetry). Same argument also proved the stereochemistry of the cis-dibutylcyclopropanone ketal. Further evidence of the cis addition/trapping is provided in the Supplementary Material. Cyclopropyl cuprates generally react with electrophiles with retention of configuration (ref 2c).